https://dx.doi.org/10.4314/WOJAST.v15i1.43

MHD CASSON FLUID FLOW WITH CHEMICAL REACTION AND SUCTION IN A POROUS MEDIUM OVER AN EXPONENTIALLY STRETCHING SHEET.

ISSN: 2141 – 3290
www.wojast.com

EKANG, I.F.[1*], JOSHUA, E.E.[1], SENGE, I.O.[2] AND NYONG, E.[1]
[1]Department of Mathematics, University of Uyo, Uyo, Nigeria
[2]Department of Mathematics, University of Benin, Benin City, Nigeria
idongesitekang@uniuyo.edu.ng, https://orcid.org/0000-0002-4014-7635

ABSTRACT

MHD Casson fluid flow with chemical reaction and suction in a porous medium over an exponentially stretching sheet was studied. The mathematical problem was solved numerically using shooting technique with fourth order Runge-Kutta method after converting the resulting partial differential equations to a system of ordinary differential equations and applying similarity transformation on the latter. The effects of some fluid parameters on the momentum and concentration profiles are examined through graphs using MATLAB. The results from the graphs show that increase in the values of Casson parameter decreases the velocity profiles and causes increase in the concentration profiles. The momentum boundary layers decrease while the solute boundary layers increase with increasing values of magnetic parameter and the permeability parameter. The concentration profile reduces with increasing values of reaction parameters.

Keywords: Casson fluid, MHD, chemical reaction, stretching sheet.

Introduction

There has been growing interest in the study of fluid flow over stretching sheets, particularly Newtonian and non-Newtonian fluids, due to their use in various industrial processes such as polymer processing and glass fiber production. The study of magnetic field effect on electrically conducting fluid is important and has various industrial applications, including magnetic materials processing, crude oil purification, and magneto hydrodynamic power generation.

(Crane, 1970) performed the first study on steady boundary layer flow caused by a linear stretching sheet. (Aly and Ebaid, 2016) examined the exact analysis for the effect of heat transfer of MHD, and radiation Marangoni boundary layer nano fluid flow past a surface embedded in a porous medium. (Turkyilmazoglu, 2016) explored the flow of a micro polar fluid due to a porous stretching sheet and heat transfer. (Jain and Choudhary, 2015) investigated the effects of MHD on boundary layer flow in a porous medium due to exponentially shrinking sheet with slip. (Reddy, 2016) discussed the MHD flow of a Casson fluid over an exponentially inclined permeable stretching surface with thermal radiation and chemical reaction.

(Ganesh *et al.*, 2018) explored Darcy-Forchheimer flow of hydromagnetic nano fluid over a stretching or shrinking sheet in a thermal stratified porous medium with second-order slip, viscous and ohmic dissipations effect. Meanwhile, (Abel *et al*., 2016) analysed MHD viscoelastic boundary layer flow and heat transfer past a convectively heated radiation stretching or shrinking sheet with temperature-dependent heat source or sink.

(Bhattacharyya *et al*., 2014) investigated dual solutions in boundary layer flow of Maxwell fluid over a porous shrinking sheet. (Chaudhary *et al*., 2016) obtained numerical solution for MHD stagnation point flow towards a stretching or shrinking surface in a saturated porous medium.

(Alam *et al*.,2016) analyzed the effects of variable fluid properties and thermophoresis on an unsteady forced convective boundary layer flow along a permeable stretching or shrinking wedge with variable Prandtl and Schmidt numbers. (Chaudhary and Chaudhary, 2016) studied the heat and mass transfer by MHD flow near the stagnation point over a stretching or shrinking sheet in a porous medium. (Ali *et al*., 2015) reported on analytical solution for fluid flow over an exponentially stretching porous sheet with surface heat flux in a porous medium by means of homotopic analysis method. (Ekang *et al*., 2021) examined MHD heat and mass flow of Nano-fluid over a non-linear permeable stretching sheet. (Senge *et al*., 2020) investigated the influence of radiation on magneto-hydrodynamics flow over an exponentially stretching sheet embedded in a thermally stratified porous medium in the presence of heat source. (Nabeela and Rashid, 2013) found solutions for non-similarity boundary layer flow in porous medium. (Mat *et al*., 2015) studied boundary layer stagnation-point slip flow and heat transfer towards a stretching or shrinking cylinder over a permeable surface. (Chakrabarti and Gupta,1979) investigated hydromagnetic flow and heat transfer over a stretching sheet. In this study, we analyze MHD Casson fluid flow with chemical reaction and suction in a porous medium over an exponentially stretching sheet. The source terms for magnetic field and porous medium are introduced on the flow.

Methods

Mathematical Formulation

Let us consider the flow of an incompressible viscous fluid past a flat sheet coinciding with the plane $y = 0$. The fluid flow is confined to $y > 0$. Two equal and opposite forces are applied along the x axis so that the wall is stretched keeping the origin fixed. The standard rheological equation of state for an isotropic and incompressible flow of a Casson fluid is

$$\tau_{ij} = \begin{cases} \left(\mu_B + \frac{p_y}{\sqrt{2\pi}}\right) 2e_{ij} \; ; & \pi > \pi_c \\ \left(\mu_B + \frac{p_y}{\sqrt{2\pi_c}}\right) 2e_{ij} \; ; & \pi < \pi_c \end{cases}$$

https://dx.doi.org/10.4314/WOJAST.v15i1.43

where $\pi = e_{ij}\, e_{ji}$ and e_{ij} is the (i,j)th component of the deformation rate, π is the product of the deformation rate with itself,π_c is the critical value of the product of the component of the rate of strain tensor with itself, μ_B is the plastic dynamic viscosity of casson fluid and p_y is the yield stress of the fluid.

$e_{ij} = \frac{1}{2}\left(\frac{\partial u_i}{\partial x_j} + \frac{\partial u_j}{\partial x_i}\right)$

The positive x coordinate is measured along the sheet and the positive y coordinate is measured perpendicular to the sheet.

The following assumptions are made to derive the governing equations; fluid suction and magnetic field are imposed at the plate surface. Let C_w be the concentration of the fluid at the surface which is assumed to be greater than the ambient concentration of the fluid, C_∞, given by

$$C_w(x) = C_\infty + C_0 e^{\frac{2x}{L}}$$

where C_∞, and C_0 are constants.

By these assumptions the governing fluid equations are as follows;

$$\frac{\partial u}{\partial x} + \frac{\partial v}{\partial x} = o \tag{1}$$

$$u\frac{\partial u}{\partial x} + v\frac{\partial u}{\partial y} = \vartheta\left(1 + \frac{1}{\beta}\right)\frac{\partial^2 u}{\partial y^2} - \frac{\sigma {\beta_0}^2}{\rho}u - \frac{\vartheta}{k}u \tag{2}$$

$$u\frac{\partial C}{\partial x} + v\frac{\partial C}{\partial y} = D\frac{\partial^2 C}{\partial y^2} - k(C - C_\infty) \tag{3}$$

where u, v are the velocity respectively in the x, y directions, ϑ is the kinematic viscosity, ρ is the fluid density (assumed to be constant), $\beta = \frac{\mu_B\sqrt{2\pi_C}}{p_y}$ is the parameter of the Casson fluid, D is the diffusion coefficient of the diffusing species in the fluid, $k = k_0 e^{\frac{x}{L}}$ is the exponential reaction rate; k_0 is a constant.

The boundary conditions are:

$$at\ y = 0,\ u = U,\ v = 0,\ C = C_w$$
$$as\ y \to \infty,\ u \to 0,\ C \to C_\infty \tag{4}$$

Here, $u = U_0 e^{\frac{x}{L}}$ is the stretching velocity, C_w is the concentration at the sheet, U_0 and C_0 are the reference velocity and reference concentration, respectively.

Now, we introduce the stream function $\varphi(x, y)$, defined by;

$$u = \frac{\partial \varphi}{\partial y}\ ,\qquad v = -\frac{\partial \varphi}{\partial x} \tag{5}$$

These automatically satisfy continuity equation. Next, introduce the similarity transformations;

$$\varphi = (2L\vartheta U_0 e^{\frac{x}{L}})^{\frac{1}{2}} f(\eta);\qquad \eta = \sqrt{\frac{U_0}{2\vartheta L}}\, e^{\frac{x}{2L}} y;\qquad \Phi = \frac{C - C_\infty}{C_0 e^{\frac{-x}{2L}}}$$

$$u = U_0 e^{\frac{x}{L}} f'(\eta);\ \ v = -\left(\frac{\vartheta U_0}{2L}\right)^{\frac{1}{2}} e^{\frac{x}{2L}}([f + \eta f'(\eta)] \tag{6}$$

Substituting the above equations into equations (2) and (7), the governing equations reduce to:

$$\left(1 + \frac{1}{\beta}\right)f''' + ff'' - 2f'^2 - (M + \lambda)f' = 0 \tag{7}$$

$$\Phi'' = Sc(\Phi' f - \Phi f' - 2\gamma\Phi) \tag{8}$$

The transformed boundary conditions are:

$$f'(0) = 1, f(0) = 0, \Phi(0) = 1, at\ \eta = 0,$$

$$f'(\eta) \to 0, \Phi(\eta) \to 0, as\ \eta \to \infty \tag{9}$$

where the prime denotes differentiation with respect to η and the dimensionless parameters are as follows:

$M = \frac{2L}{U_0}\frac{\sigma {\beta_0}^2}{\rho} e^{-\frac{x}{L}}$ is the Magnetic parameter

$\lambda = \frac{2L}{U_0}\frac{\vartheta}{k} e^{-\frac{x}{L}}$ is the permeability parameter

$Sc = \frac{\vartheta}{D}$ is the Schmidt number

$\gamma = \frac{k_0 L}{U_0}$ is the reaction rate parameter, where $\gamma > 0, \gamma = 0, \gamma < 0$ is the destructive reaction, absence of reaction and generative reaction respectively.

Hence the dimensionless form of Skin friction (C_f) and the Local Nusselt number (Nu_x) are given by;

$$C_f\left(\frac{2L}{x}\right)^{\frac{1}{2}}\left(Re_x{}^{\frac{1}{2}}\right) = \left(1 + \frac{1}{\beta}\right)f''(0);$$

$$Sh_x = \left(\frac{2L}{x}\right)^{\frac{1}{2}} Re_x{}^{-\frac{1}{2}}(-\Phi'(0)) \tag{10}$$

where $Re_x = \frac{xU_w}{\vartheta}$ is the local Reynolds number.

Numerical Solution

The dimensionless equations (7) and (8) subject to the boundary conditions (9) are nonlinear equations, hence solving numerically, we convert them to a system of equations by setting the following:

Let

$$\begin{pmatrix} y_1 \\ y_2 \\ y_3 \\ y_4 \\ y_5 \\ y_6 \end{pmatrix} = \begin{pmatrix} \eta \\ f \\ f' \\ f'' \\ \Phi \\ \Phi' \end{pmatrix} \tag{11}$$

$$\begin{pmatrix} y_1' \\ y_2' \\ y_3' \\ y_4' \\ y_5' \\ y_6' \end{pmatrix} = \begin{pmatrix} 1 \\ y_3 \\ y_4 \\ f''' \\ y_6 \\ \Phi'' \end{pmatrix} \tag{12}$$

where

$$f''' = \left(1 + \frac{1}{\beta}\right)\{-y_2 y_4 + 2{y_3}^2 + (M + \lambda)y_3\}$$

$$\phi'' = Sc[-y_2 y_6 + y_3 y_5 + 2\gamma y_5],$$

satisfying

$$\begin{pmatrix} y_1(0) \\ y_2(0) \\ y_3(0) \\ y_4(0) \\ y_5(0) \\ y_6(0) \end{pmatrix} = \begin{pmatrix} 0 \\ 0 \\ 1 \\ A_1 \\ 1 \\ A_2 \end{pmatrix} \tag{13}$$

https://dx.doi.org/10.4314/WOJAST.v15i1.43

where, A_1 and A_2 are guessed such that

$$\begin{bmatrix} y_3(\infty) \\ y_4(\infty) \end{bmatrix} = \begin{bmatrix} 0 \\ 0 \end{bmatrix} \qquad \text{as } \eta \to \infty$$

These equations are solved numerically using shooting technique with fourth order Runge-Kutta method. The boundary condition as $\eta \to \infty$ was replaced by a finite value in accordance with standard practice in the boundary layer analysis. We set $\eta_\infty = 10$

Results and Discussion

The effects of the dimensionless governing parameters namely: Casson parameter (β), Schmidt number (Sc), magnetic parameter (M), permeability parameter (λ) and Reaction rate parameter (γ) on the velocity and temperature distribution profiles are analyzed numerically using the method mentioned in the previous section. To do this, we set the fluid properties to be constant. Numerical values are generated and using MATLAB, the following graphs are plotted by varying the fluid properties with basics at: $\beta = 2.0,\ M = 0.5,\ \lambda = 0.2,\ Sc = 1.0, \Upsilon = 0$

Figure 1 depicts the effect of Casson parameter β on velocity profiles. The velocity profile decreases as the Casson parameter (β) value increases. The Casson parameter produces a resistance in the fluid flow and consequently the boundary layer thickness decreases for higher value of Casson parameter.

Figures 2, 3, 4 show the effect of Casson parameter β on concentration profiles. Increasing the values of the Casson parameter β increases the concentration profiles and the solute boundary layer thickness. It is noted that the effect of β is much more pronounced in the case of constructive chemical reaction.

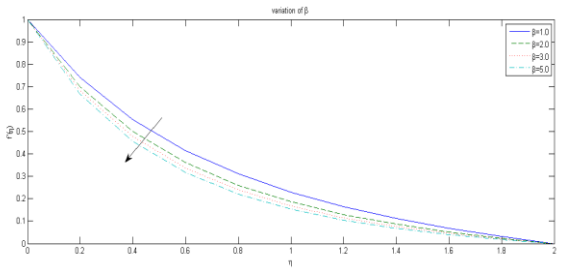

Figure 1: Variation of velocity, $f'(\eta)$ with η for several values of β

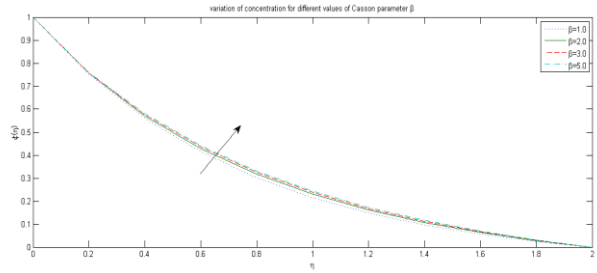

Figure 2: Variation of concentration, $\Phi(\eta)$ with η for several values of β when γ=0 (absence of reaction)

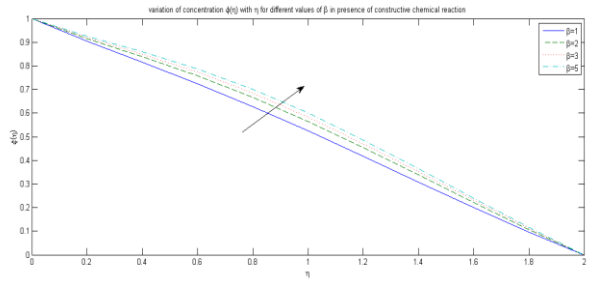

Figure 3: Variation of concentration, $\Phi(\eta)$ with η for several values of β when $\gamma < 0$

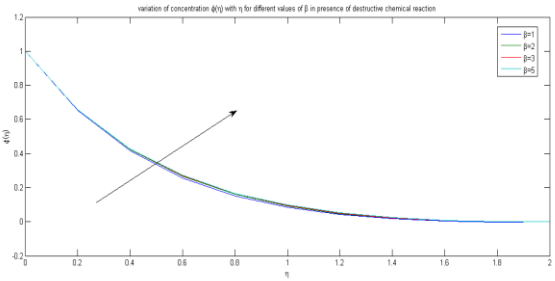

Figure 4: Variation of concentration, $\Phi(\eta)$ with η for several values of β when $\gamma > 0$

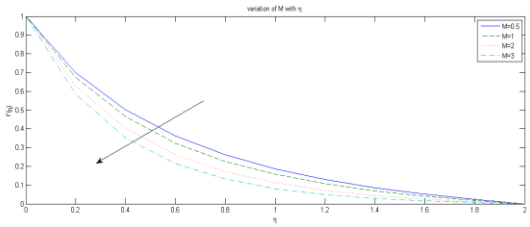

Figure 5: Variation of velocity, $f'(\eta)$ with η for several values of M

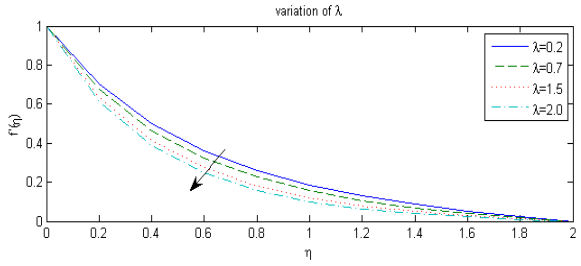

Figure 6: Variation of velocity, $f'(\eta)$ with η for several values of λ

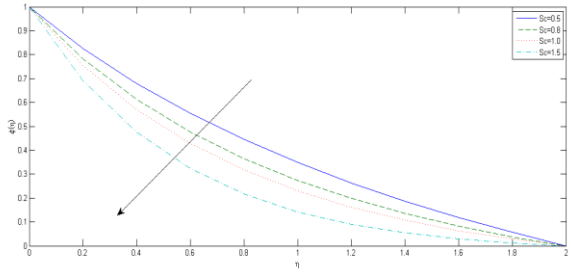

Figure 7: Variation of concentration $\Phi(\eta)$ with η for different values of Sc in the absence of chemical reaction (γ=0)

https://dx.doi.org/10.4314/WOJAST.v15i1.43

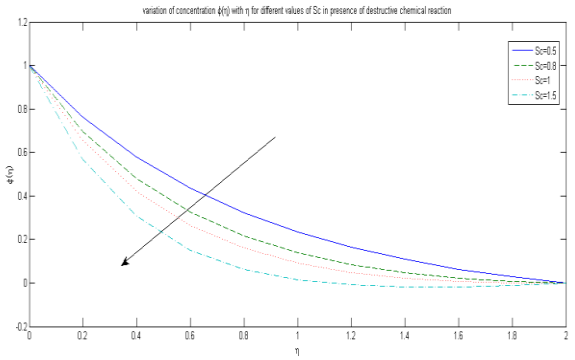

Figure 8: Variation of concentration $\Phi(\eta)$ with η for different values of Sc when γ>0

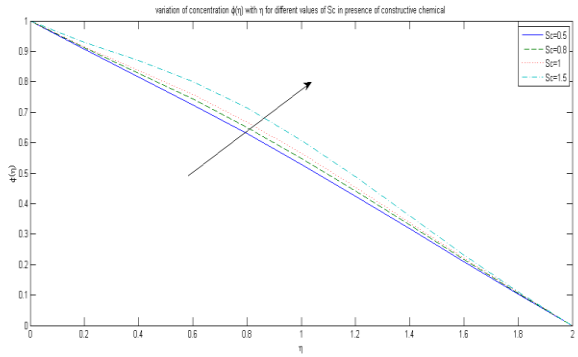

Figure 9: Variation of concentration $\Phi(\eta)$ with η for different values of Sc when γ<0

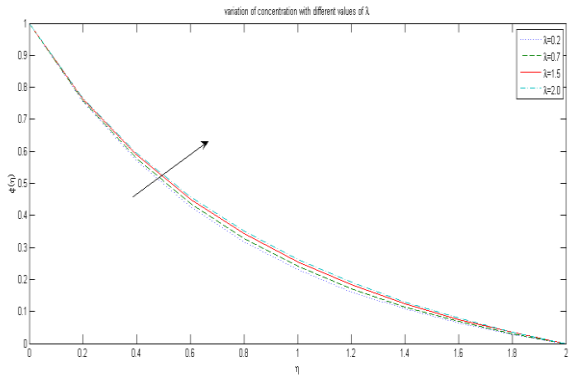

Figure 10: Variation of concentration $\Phi(\eta)$ with η for different values of λ

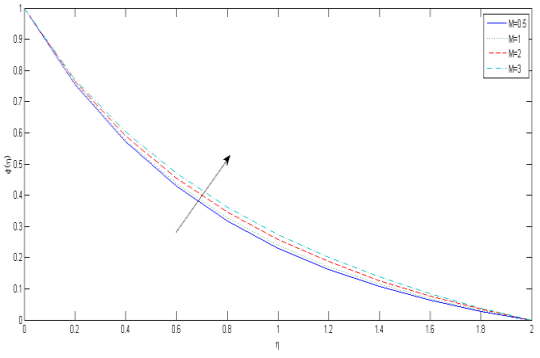

Figure 11: Variation of concentration $\Phi(\eta)$ with η for different values of M

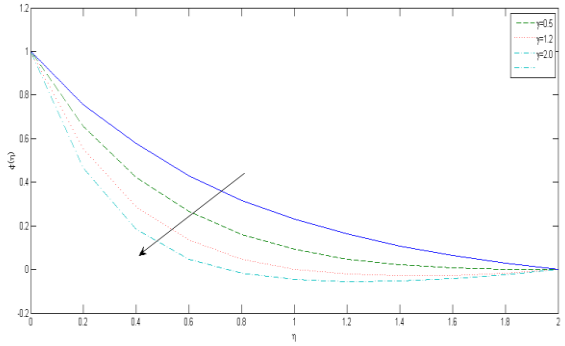

Figure 12: Variation of concentration Φ (□) with □ for different values of γ

Figures 5 and 6 display the influence of magnetic parameter, M, and the permeability parameter, λ, on the velocity profiles respectively. The velocity profiles and momentum boundary layers decrease with increasing values of magnetic and permeability parameters.

Figures 7 and 8 show the effect of Schmidt number on concentration in the absence of chemical reaction (when $\gamma = 0$) and the presence of destructive chemical reaction (when $\gamma > 0$). The concentration profiles decrease with increasing values of Schmidt number. The reaction rate parameter is a decelerating agent and as a result the solute boundary layer becomes thinner. Figure 9 shows the nature of the concentration profiles for different values of Schmidt number in the presence of constructive reaction (when $\gamma < 0$). An increase in Schmidt number increases the solute boundary layer thickness. Here, it is observed that the concentration profiles increase as the values of the Schmidt number increase.

Figures 10 and 11 examine the effect of magnetic parameter, M, and the permeability parameter, λ, on the concentration profiles respectively. Increasing the values of magnetic parameter, M, and the permeability parameter, λ, increases the concentration profiles and the solute boundary layers.
Figure 12 displays the rate of reaction γ against concentration profiles. It is found that as γ increases, concentration reduces. It is noted that the reaction rate parameter is a decelerating agent, as a result, the concentration boundary layer decreases.

Conclusion

The effects of the fluid parameters on the heat transfer are examined with the help of graphs. From the graph we can see that increase in the values of Casson parameter, decreases the velocity profiles and causes increase in the concentration profiles. The momentum boundary layers decreases while the solute boundary layers increase with increasing values of magnetic parameter and the permeability parameter. The concentration profile reduces with increasing values of reaction rate parameters. The solute boundary layers decrease with increasing values of Schmidt number in the absence of chemical reaction and the presence of destructive chemical reaction while they increase in the presence of constructive chemical reaction.

Notations

Notations used in the work are;
η : Viscosity of the fluid
μ: Magnetic permeability
ρ: Density of the fluid
σ: Electrical conductivity of the fluid
ϑ: Kinematic viscosity of the fluid
λ: Permeability parameter of the fluid
γ: Chemical reaction rate of the fluid
S: Suction parameter
Re: Reynolds number
Nu: Nusselt number
C_f: Skin friction

References

Abel, M.S., Mahabaleshwar, U.S. and Mahesh, K.B. (2016). MHD Viscoelastic Boundary Layer Flow and Heat Transfer Past a Convectively Heated Radiating Stretching/Shrinking Sheet with Temperature Dependent Heat Source/Sink. *International Journal of Physics and Mathematical Sciences*, 6(1): 50-62.

Alam, M.S., Khatun, M.A., Rahman, M.M. and Vajravelu, K. (2016). Effects of Variable Fluid Properties and Thermophoresis on Unsteady Forced Convective Boundary Layer Flow along a Permeable Stretching/shrinking wedge with Variable Prandtl and Schmidt numbers, *International Journal of Mechanical Sciences*, 105: 191-205.

Ali, A., Zaman, H., Abidin, M.Z. and Shah, S.I.A. (2015). Analytic Solution for Fluid Flow over an Exponentially Stretching Porous Sheet with Surface Heat Flux in Porous Medium by means of Homotopy Analysis Method. *American Journal of Computational Mathematics*, 5(02): 224.

Aly, E.H. and Ebaid, A. (2016). Exact analysis for the effect of heat transfer on MHD and radiation Marangoni boundary layer nanofluid flow past a surface embedded in a porous medium. *Journal of Molecular liquids*, 215: 625-639.

Bhattacharyya, K., Hayat, T. and Alsaedi, A. (2014). Dual solutions in Boundary Layer Flow of Maxwell Fluid over a Porous Shrinking Sheet. *Chinese Physics B*, *23*(12): 124701.

Chakrabarti, A. and Gupta, A.S. (1979). Hydromagnetic Flow and Heat Transfer over a Stretching Sheet. *Quarterly of Applied Mathematics*, 37(1): 73-78.

Chaudhary, S. and Choudhary, M.K. (2016). Heat and mass transfer by MHD flow near the stagnation point over a stretching or shrinking sheet in a porous medium. *Indian Journal of Pure and Applied Physics*, 54(3): 209-217.

Chaudhary, S., Singh, S. and Chaudhary, S. (2016). Numerical Solution for Magnetohydrodynamic Stagnation Point Flow towards a Stretching or Shrinking Surface in a Saturated Porous Medium. *International Journal of Pure and Applied Mathematics*, 106(1): 141-155.

Crane, L. J. (1970). Flow Past a Stretching Plate, *Zeitschrift für Angewandte Mathematik und Physik* (ZAMP) 21: 645-647.

Ekang, I. F., Joshua, E. E., Senge, I. O. and Nwachukwu, O. O., (2021). MHD Heat and Mass flow of Nano-fluid over a Non-linear Permeable Stretching Sheet, *Journal of Mathematics and Computer Science*, 11(5): 5196-5212.

Ganesh, N.V., Hakeem, A.A. and Ganga, B., (2018). Darcy–Forchheimer Flow of Hydromagnetic Nanofluid over a Stretching/shrinking sheet in a Thermally Stratified Porous medium with Second order slip, Viscous and Ohmic Dissipations Effects. *Ain Shams Engineering Journal*, *9*(4), 939-951.

Jain, S. and Choudhary, R. (2015). Effects on MHD on boundary layer flow in Porous Medium due to Exponentially Shrinking sheet with Slip, *Procedia Engineering Journal*, 127: 1203-1210.

Mat, N., Arifin, N., Nazar, R. and Bachok, N. (2015). Boundary Layer Stagnation-Point Slip Flow and Heat Transfer towards a Shrinking/Stretching Cylinder over a Permeable Surface. *Applied Mathematics*, 6: 466-475.

Nabeela K. and Rashid, M. (2013). Solutions of non-similarity boundary layer flow in porous medium, *Applied Mathematics*, 4: *127-136.*

Reddy, P.B.A., (2016). Magnetohydrodynamic flow of a Casson fluid over an exponentially inclined permeable stretching surface with thermal radiation and chemical reaction. *Ain Shams Engineering Journal*, 7(2): 593-602.

Senge, I. O., Oghre, E. O., Ekang, I. F., (2020). Influence of Radiation on Magneto-hydrodynamics Flow over an Exponentially Stretching Sheet Embedded in a Thermally Stratified Porous Medium in the Presence of Heat Source, *Earthline Journal Mathematical Science*, 5: 345-363.

Turkyilmazoglu, M., (2016). Flow of a micropolar fluid due to a porous stretching sheet and heat transfer. *International Journal of Non-Linear Mechanics*, 83: 59-64.